Malaysian Journal of Soil Science 2022 Vol. 26: 55-72

Modelling Soil-Water Behavior in Oil Palm Plantations Using Neutron Moisture Meter (NMM) and Resistivity Imaging System (RIS)

Rajoo, K.S.[1,2*], Yusop, Z.[3], Mejus, L.[4] and Gerusu, G.J. [1,2*]

[1] Department of Forestry Science, Faculty of Agricultural Science and Forestry, Universiti Putra Malaysia Bintulu Sarawak Campus, 97000 Bintulu, Sarawak
[2] Institute of Ecosystem Science Borneo, UPM Bintulu Sarawak Campus, Jalan Nyabau, 97000 Bintulu, Sarawak.
[3] Institute of Environmental and Water Resources Management (IPASA),
[4] Waste and Environmental Technology Division, Malaysian Nuclear Agency, Bangi, 43000 Kajang, Selangor, Malaysia.

**Corresponding author: keeren.rajoo@upm.edu.my*

ABSTRACT

Water management is rarely a focus in Southeast Asian oil palm plantations, due to high rainfall all year long. However, this climatic condition is changing. There is increasing evidence that climate change is causing tropical regions to have reduced annual mean precipitation and increased prevalence of dry seasons. Thus, knowledge gaps in the area of soil-water relationship in these agricultural systems will result in inefficient water management. Therefore, this study was conducted to evaluate the potential of two approaches in monitoring and modelling soil water behaviour under oil palm canopies. The first approach used Neutron Moisture Meter (NMM), to obtain a time series on Θ, including evaluating soil-rainfall relationship. The second approach used Resistivity Imaging System (RIS), to provide data on stratigraphy that was used to further characterize the geologic setting of soil (6 m depth) and its effects on soil moisture. The results revealed a small significant variability in Θ values in the 20 different soil depths. Θ values also showed significant increases in response to high rainfall events (>30.0 mm) which decreased with time. Soil-water content percentage changes ranged from 9.5 to 23.8% at different depths. The resistivity imaging surveys successfully mapped the soil water content underneath the oil palm catchment up to 6 m depth, revealing leakages to groundwater flow at some study sites. Both techniques (NMM and RIS) were able to model the soil-water relationship in oil palm plantations. These methods can be used to charter better water management strategies in oil palm plantations in the future.

Key words: **Soil water content, soil stratigraphy pattern, Resistivity Imaging System, oil palm catchment**

INTRODUCTION

Oil palm is a vital socio-economic crop since it produces the most widely consumed vegetable oil in the world (Gonzalez-Diaz *et al.* 2021). This plantation crop grows well in high temperatures and requires large amounts of water, making it an ideal crop for tropical climates (Rajoo *et al*. 2021a). It is therefore no surprise that Indonesia and Malaysia are the world's largest producers of palm oil. In 2017, Malaysia produced 39% of the world's palm oil, which came from 5.81 million hectares of oil palm plantations (Olaniyi and Szulczyk 2020). Due to ever increasing demand for edible oils, it is very likely that palm oil production will continue to rise for the foreseeable future (Saad *et al.* 2021).

The demand for palm oil has fueled research interest in this field. However, these studies usually focus on sustainability (Anyaoha *et al*. 2018) and managing by-products or

waste from palm oil production (Gonzalez-Diaz *et al.* 2021; Saad *et al.* 2021; Karam *et al.* 2022). There is also growing research interest in palm oil certification (Tey *et al*. 2021) and evaluating the social impacts of palm oil production (Castellanos-Navarrete *et al*. 2021). Unfortunately, research pertaining to water demand and soil water content in oil palm plantations is almost non-existent (Tezara *et al.* 2021), especially in the Southeast Asia (Subramaniam and Hashim 2018), the world's largest producer of palm oil.

Agricultural production is the biggest user of freshwater, with over 70% of global freshwater being used in this area (Li *et al*. 2021). This demand for freshwater is only going to increase since by 2050, the world's population will exceed 9 billion, requiring an estimated 50% increase in agricultural production (Li *et al*. 2021). Therefore, water management is an integral part of agricultural production, especially in non-tropical regions. Quantification of soil water contents (Ɵ) has long been known to be essential in agricultural systems. Rawls *et al.* (1973) reported that the amount of Ɵ in the soil has an impact on vegetative yield. For instance, in western Kenya, Radersma and Ong (2004) reported that a soil-water content reduction of 2 to 3% caused a 40% decrease in maize-production.

Water management is rarely a focus in tropical agricultural systems, due to high rainfall all year long (Subramaniam and Hashim 2018; Rajoo *et al.* 2020). However, this climatic condition is changing. There is increasing evidence that climate change is affecting tropical regions (Rajoo et al., 2021b), namely by reducing annual mean precipitation and increased prevalence of dry seasons (Dinar *et al*. 2019). This has contributed to water scarcity, affecting oil palm production (Subramaniam and Hashim 2018; Tezara *et al*. 2021). It is likely that irrigation systems will soon be required for oil palm plantations, perhaps because knowledge gaps in the area of soil-water relationship in oil palm plantations will result in inefficient water management in these agricultural systems.

Therefore, this study aims to evaluate the potential of two approaches in monitoring and modelling soil water content under oil palm canopies. The first approach used Neutron Moisture Meter (NMM). NMM was used to obtain a time series on Ɵ, including evaluating the soil-rainfall relationship in oil palm plantations. The second approach used Resistivity Imaging System (RIS) to provide data on stratigraphy that was used to further characterize the geologic setting of soil (6 m depth) and its effects on soil moisture. The availability of adequate soil water in the root zone has a large impact on plant growth and biomass production, thus RIS will provide essential data in this area. To date, there has been no study using NMM and RIS to evaluate the soil-water relationship in oil palm plantations. Thus, this study will provide a better understanding of Ɵ characteristics, stratigraphy pattern and their effects on soil water content in oil palm plantations. This will allow for a more reliable methodology for future water management strategies in oil palm plantations.

MATERIALS AND METHODS

Study Location

This study was carried out at three catchments in Sedenak oil palm plantation, Johor, Malaysia (*Figure 1*). These undulating areas have an altitude ranging from 43 to 62 m above sea level and are situated in the upstream of the Skudai River, approximately at 01^{o} 43' 35" N and 103^{o} 32' 42" E. The general physical characteristics of these catchments are summarized in Table 1. These sites were planted with *Elaeis guineensis Jacq* clones PAMOL/FELDA. The canopy cover is quite uniform ranging from 85% to 90% of the ground area. All three

study sites had a density of 148 ha^{-1} (planting distance: 8 X 8 m), with leaf area index (LAI) of 5.9 to 7.1. LAI increases with palm age and reaches a stable maximum after 10 years, thus the LAI at the study sites were at their maximum.

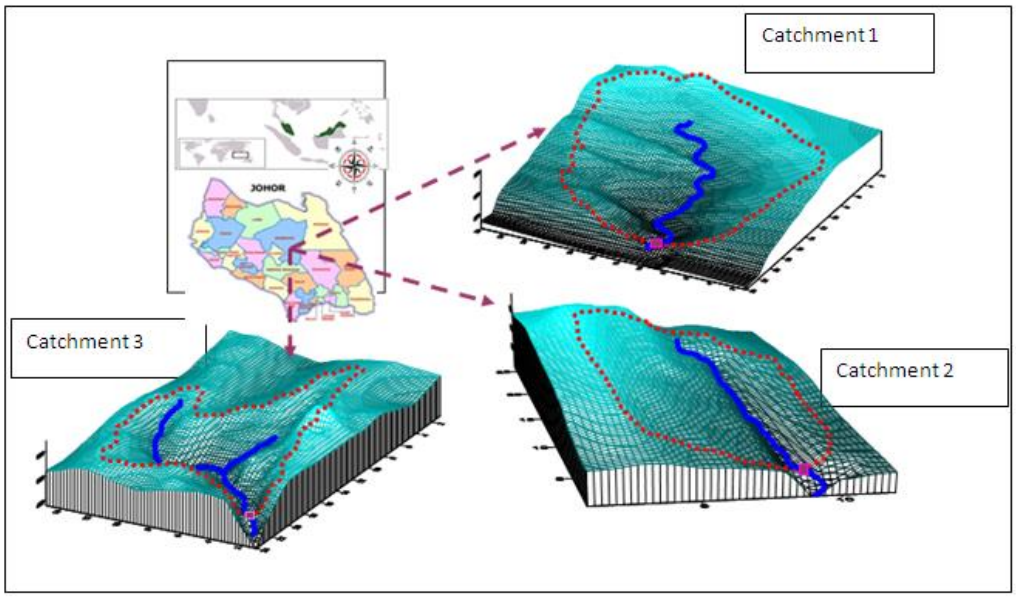

Figure 1: Location of study sites

TABLE 1
Summary of physical characteristics of the study catchments

Catchment	C1	C2	C3
Location	Sedenak Estate, Johor	Sedenak Estate, Johor	Sedenak Estate, Johor
GPS point	approx 01º 44' 37" N and 103º 32' 41" E	approx 01° 42' 54" N and 103° 31' 47" E	approx 01º 43' 35" N and 103º 32' 42" E
Oil palm clone	PAMOL/FELDA (<3 years old)	PAMOL/FELDA (5-6 years old)	PAMOL/FELDA (11 years old)
Topography	undulating area	undulating area	undulating area
Soil texture	Coarse sandy clay loam of red yellow ultisols and belongs to Rengam series	Coarse sandy clay loam of red yellow ultisols and belongs to Rengam series	Coarse sandy clay loam of red yellow ultisols and belongs to Rengam series
Total area (ha)	17.59	8.17	15.62
Stream length (m)	351	153	641
Stream max. elevation (masl)	66.7	58.8	60.9
Stream min. elevation (masl)	55.4	49.0	43.5
Stream slope	0.0321	0.0637	0.0271
Stream slope (%)	9	7	8
Catchment length (m)	372	221	705
Catchment max. elevation (masl)	67.9	63.1	62.8
Catchment min. elevation (masl)	55.4	49.0	43.5
Mean catchment slope (m/m)	0.0356	0.0916	0.0300

Rainfall Measurements

An automatic tipping bucket rain gauge (ONSET RG2-M) was installed at all study sites. ONSET RG2-M rain gauge logs readings cumulatively whenever the tipping bucket is filled with 0.2 mm rainwater. The rain gauge was installed at an open area within the catchment with enough clearance above a 45^{o} angle from the edge of the gauge. Rainfall data was retrieved on a weekly basis using a laptop.

Soil Survey

A detailed investigation on soil type and bedrock depth profile was conducted at three selected sampling points (BH1, BH2 and BH3) within Catchment 3 (*Figure 2*). A Mackintosh Probe was used to investigate the site. This soil sampling equipment used a 4.5-kilogram hammer to determine the number of blows required for every 30 cm penetration. The probing was terminated when the blow count of 400 (refusal) was recorded over a penetration of 300 mm or less. For this study, the average penetration refusal or stop for BH1, BH2 and BH3 were 1.55 m, 2.05 m and 4.95 m, respectively.

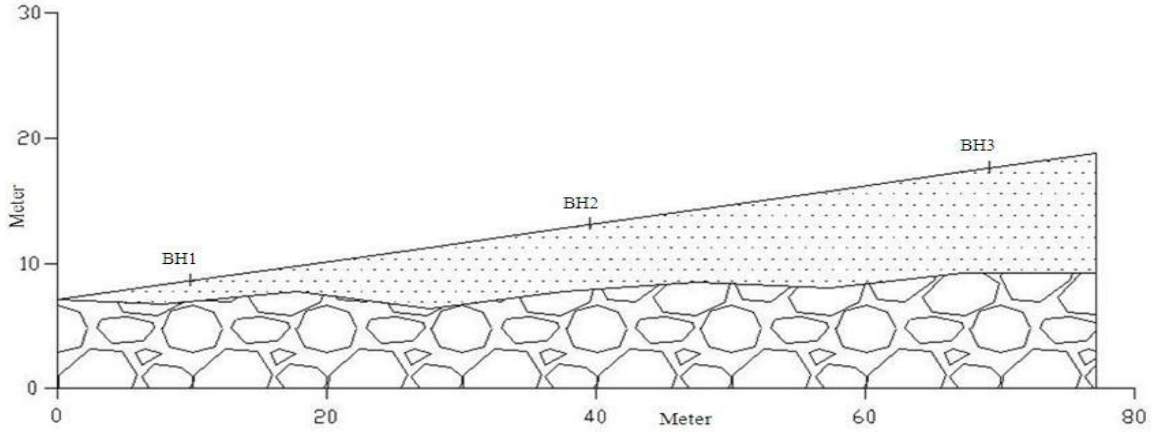

Figure 2: Soil survey locations

Neutron Moisture Meter (NMM) Sampling

The NMM used in this study was manufactured by Didcot Instrument Company Limited, Abingdon, Oxon, England. The neutrons, emitted 50-mCi from its source (241Am-Be), are radioactive and reflect on collision with particles of equal mass (hydrogen nuclei). The thermalized neutrons are detected by a BF3 detector (*Figure 3*). In water the NMM gave ~ 1200 count per second (c.p.s). Access tubes of 2-m depth for these measurements were installed at the three selected sampling points (BH1, BH2, BH3) in Catchment 3. Temporal changes of soil water content (Θ) was carried out 39 times at these sampling points for a period of three months (Oct to Dec), by measuring the count rates of the neutron meter and gravimetric soil water contents at 20 different depths: 0.10, 0.20, 0.30, 0.40, 0.50, 0.60, 0.70, 0.80, 0.90, 1.00, 1.10, 1.20, 1.30, 1.40, 1.50, 1.60, 1.70, 1.80, 1.90 and 2.00 m.

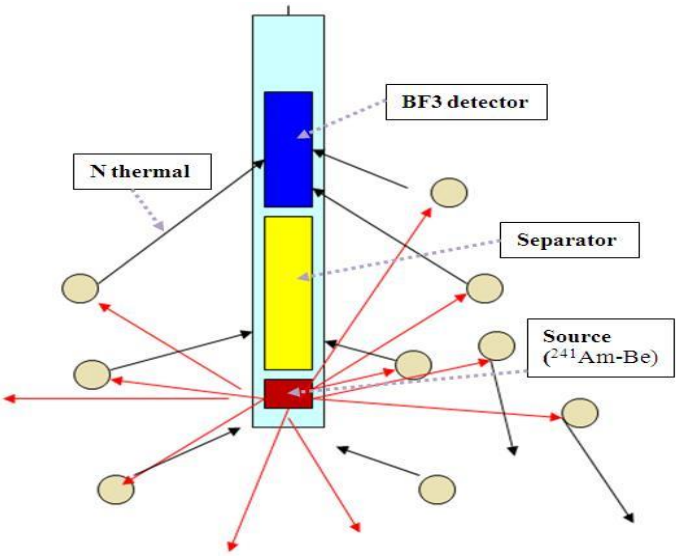

Figure 3: The NMM probe

Soil samples to determine mean value of the soil water content based on gravimetric method were retrieved horizontally at appropriate depths in cores adjacent to neutron access tubes. Core samples of 100 cm^3 from each depth were collected and sealed in plastic begs for further analysis in the laboratory. All samples collected were weighed moist, oven-dried for 4 days at 105°C, and weighed dry. The relationship between gravimetric water content and neutron meter readings is defined as follows (Chanasyk and Naeth 1996):

$$CR = \left(\frac{CR_{soil}}{CR_{water}}\right) \times 100(\%)$$

where
CR_{soil} = counts s^{-1} in soil
CR_{water} = counts s^{-1} in water tank

Then the gravimetric water content, W, (%) is

$$W = aCR + b(\%)$$

where
a and *b* are constants.

The calibration equation retrieved from the relationship between gravimetric water content and neutron meter readings strongly correlated with coefficient of determination (r2) of 0.88 (*Figure 4*). This suggests that soil water content (Θ) at the study site can be measured using NMM by using the following linear least-square regression equations:

$$\Theta = 0.0582(NMM_{reading}) - 0.125; \qquad r^2 = 0.88$$

where
Θ – soil water content (%);$NMM_{reading}$ – neutron count/second

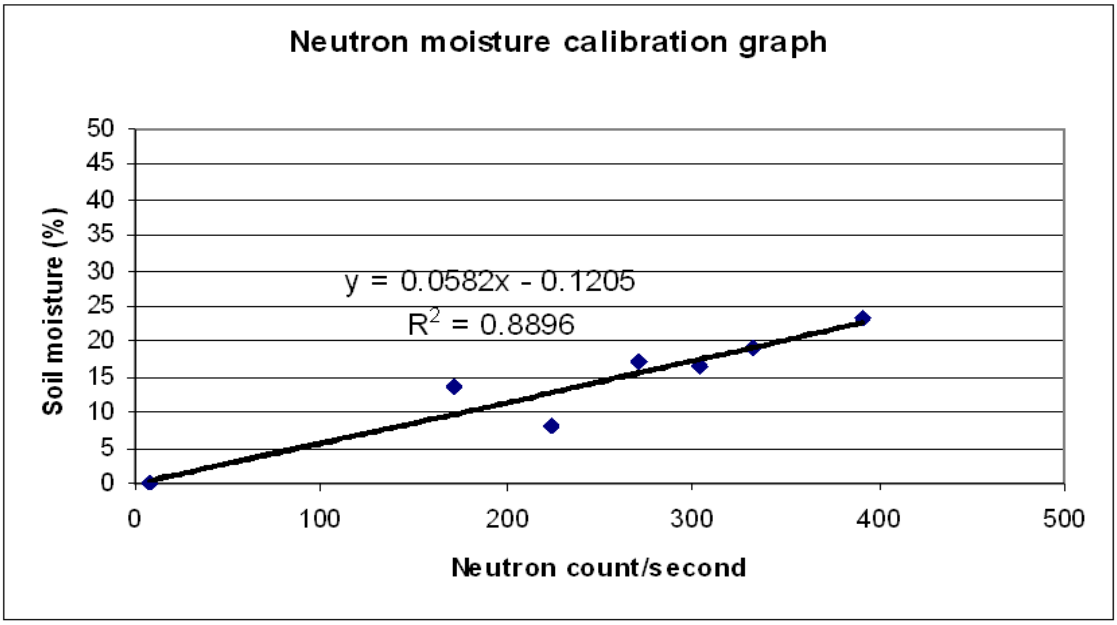

Figure 4: Calibration curve

Resistivity Imaging System (RIS) Sampling

RIS sampling was conducted at all three catchments (C1. C2 and C3) using ABEM Terrameter SAS4000 connected to LUND electrode selector 464 system (ES464). This system uses a four electrode dipole–dipole type array with 2 m electrode spacing and four dipole offset. A continuous sequence of measurements (with 1480 total measurements) was made covering a total length of approximately 160 m, providing a maximum imaged depth of about 6 m (*Figure 5*).

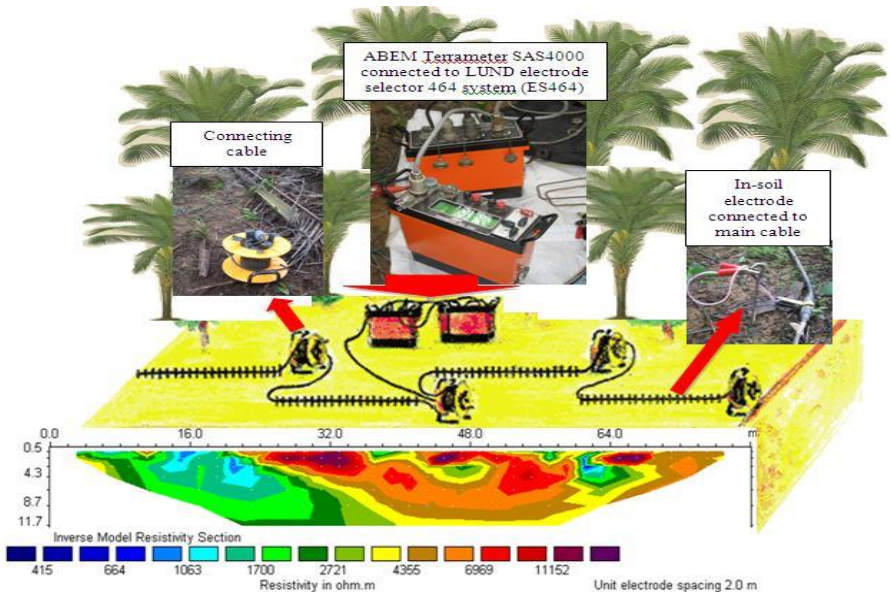

Figure 5: General setup of resistivity imaging monitoring system at the study sties

Resistivity measurements were based on the principle that the distribution of electrical potential in the ground around a current-carrying electrode depends on the electrical resistivities and distribution of the surrounding soils and rocks. Subsurface resistivity is measured by applying an electric current through two electrodes and measuring the resulting voltage difference between two potential electrodes. The measurement is reported as apparent resistivity (ρ_a)

$$\rho_a = \frac{kV}{I}$$

where V is the measured voltage difference, I is the applied current, and k is a geometric factor based on the electrode arrangement (Loke 2000).

The field measurements of apparent resistivity were calculated by multiplying the resistance value of geometric correction which is based on the arrangement of the current electrode and the potential electrode in relation to each other (Ain-Llhout *et al*. 2016; Pan *et al*. 2021).

To estimate true resistivity, the apparent resistivity data files are then inverted using the commercial interpretation software RES2DINV (Rucker *et al.* 2021). The program uses a nonlinear least squares optimization technique to obtain the inversion of apparent resistivities (Pan *et al*. 2021). The results from this program were used to generate 2D sections of resistivity data referred to as inverted field datasets or inversion results. The inversion results were used to characterize the resistivity changes in the vertical direction, as well as in the horizontal direction along the survey line (Loke 2000). Resistivity is measured in ohm-m or ohm-ft, and is the reciprocal of the conductivity of the material.

RESULTS AND DISCUSSION

Soil Water Changes According to Time and Depth

As mentioned previously, temporal changes of soil water content (Θ) under oil palm canopy were estimated from 39 individual events using the Neutron Moisture Meter (NMM). All Θ data from 20 different depths were analyzed accordingly: 0.10, 0.20, 0.30, 0.40, 0.50, 0.60, 0.70, 0.80, 0.90, 1.00, 1.10, 1.20, 1.30, 1.40, 1.50, 1.60, 1.70, 1.80, 1.90 and 2.00 m. The summarised results retrieved from the three different access-tube locations at the study sites are shown in Table 2 and *Figure 6.*

TABLE 2
Summary of Θ values of BH1, BH2 and BH3

SOIL DEPTH	Θ (%) for BH1		Θ (%) for BH2		Θ (%) for BH3	
	Values range*	Average	Values range*	Average	Values range*	Average
200	20-27	24	20-27	23	23-28	25
190	20-27	23	21-27	22	22-28	25
180	20-26	23	20-26	22	22-28	24
170	19-25	22	20-25	22	21-27	23
160	19-25	22	20-25	22	21-28	24
150	18-25	22	20-25	22	21-28	23
140	18-25	22	20-26	21	21-27	23
130	16-24	21	19-25	21	20-27	23
120	16-24	21	19-25	21	20-26	22
110	17-26	22	19-24	21	20-25	22
100	17-26	22	18-23	21	19-25	22
90	16-26	21	16-24	20	18-25	21
80	15-25	20	16-22	20	18-24	21
70	13-24	19	17-23	20	18-24	21
60	15-24	19	15-22	20	17-24	20
50	14-24	18	15-21	19	16-23	20
40	13-22	17	14-21	19	15-22	19
30	12-20	16	13-20	18	14-22	18
20	12-19	15	12-21	17	12-21	17
10	7-14	10	8-16	12	6-17	10
Average	15.9-23.9	20	17.1-23.4	20	18.2-25.0	21

*Note : *-data ranges based on 39 measurement events*

The Θ values obtained ranged from 7 to 27%, 8 to 27% and 6 to 28% for BH1, BH2 and BH3, respectively. The upper layers of 0.8, 0.6 and 0.5 m soil depth showed Θ values ranging from 20 to 28%, indicating moderate wet and wet soil conditions for BH1, BH2 and BH3, respectively. However, the overall Θ average at 2.0 m depth within the study area suggested a moderate wet soil. The general descriptive statistics of all three access tubes of Θ data are presented in Table 3. Further details of the distribution pattern of soil water content can be observed in the box plot in *Figure 7*. The data reveals a tail towards the smaller value indicting it is negatively skewed.

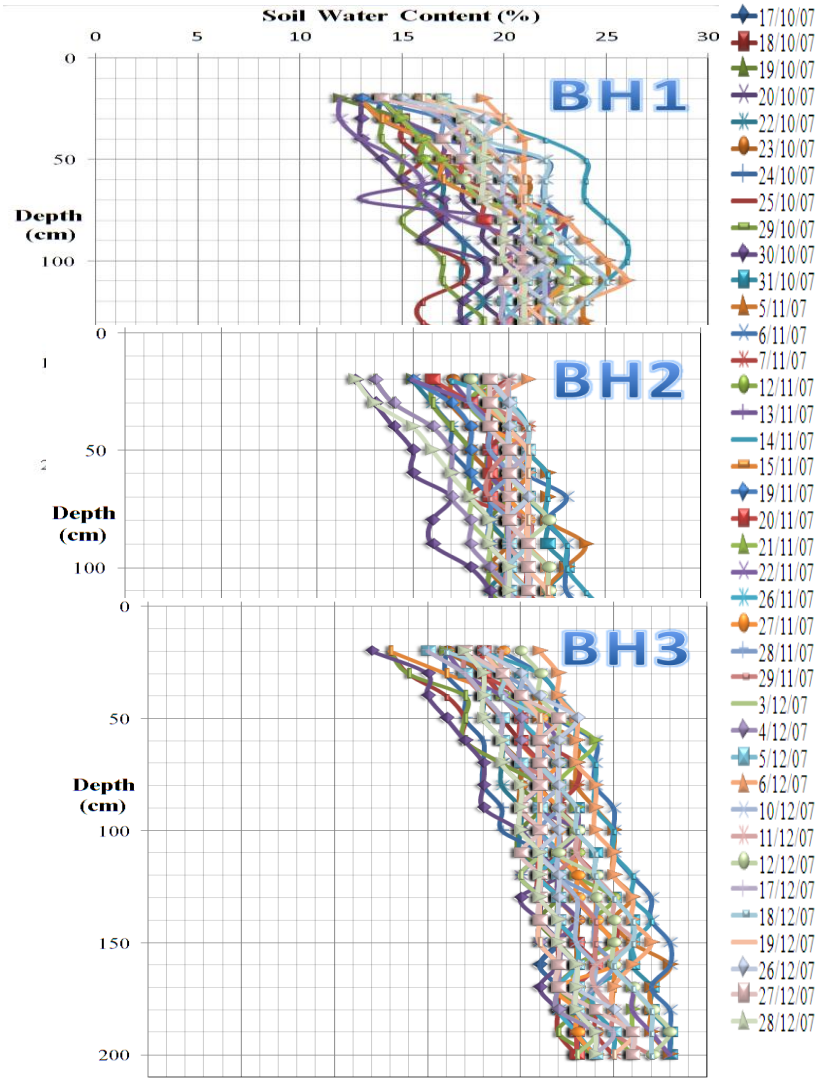

Figure 6: Characteristics of Θ for BH1, BH2 and BH3

TABLE 3
Summary of soil water content (%) descriptive analysis for bore holes 1, 2 and 3 (39 events)

		Bore Hole 1			Bore Hole 2			Bore Hole 3		
		Oct	Nov	Dec	Oct	Nov	Dec	Oct	Nov	Dec
	No of events	11	15	13	11	15	13	11	15	13
Range of values	Mean	17.1-21.1	18.8-23.1	19.7-22.6	17.8-22.0	19.0-22.5	17.9-21.9	18.8-23.1	20.5-24.5	19.9-23.9
	Standard error	0.56-0.83	0.57-1.02	0.47-0.87	0.37-0.81	0.41-0.84	0.31-0.76	0.61-0.94	0.60-1.06	0.58-0.89
	Median	17-22	20-24	20-24	19-23	20-23	19-22	20-24	21-25	20-25
	Mode	15-23	20-25	20-25	19-23	20.24	20.24	20-26	21-28	21-27
	Standard Deviation	2.52-3.73	2.56-4.56	2.12-3.90	1.67-3.63	1.82-3.76	1.39-3.42	2.72-4.19	2.67-4.74	2.60-3.96
	Sample variance	6.36-13.94	6.58-20.80	4.48-15.21	2.79-13.14	3.31-14.16	1.94-11.69	7.41-17.57	7.15-22.46	6.75-15.69
	Minimum	9-10	9-12	7-14	9-14	9-14	8-16	8-12	6-12	7-17
	Maximum	21-25	22-26	22-26	22-27	22-26	21-26	23-28	24-28	24-28
	Sum	335-421	376-462	394-451	355-440	380-449	357-438	376-462	413-490	398-478
	Confidence Level(95.0%)	1.18-1.75	1.20-2.13	0.99-1.83	0.78-1.70	0.85-1.76	0.65-1.60	1.27-1.98	1.25-2.20	1.22-1.85

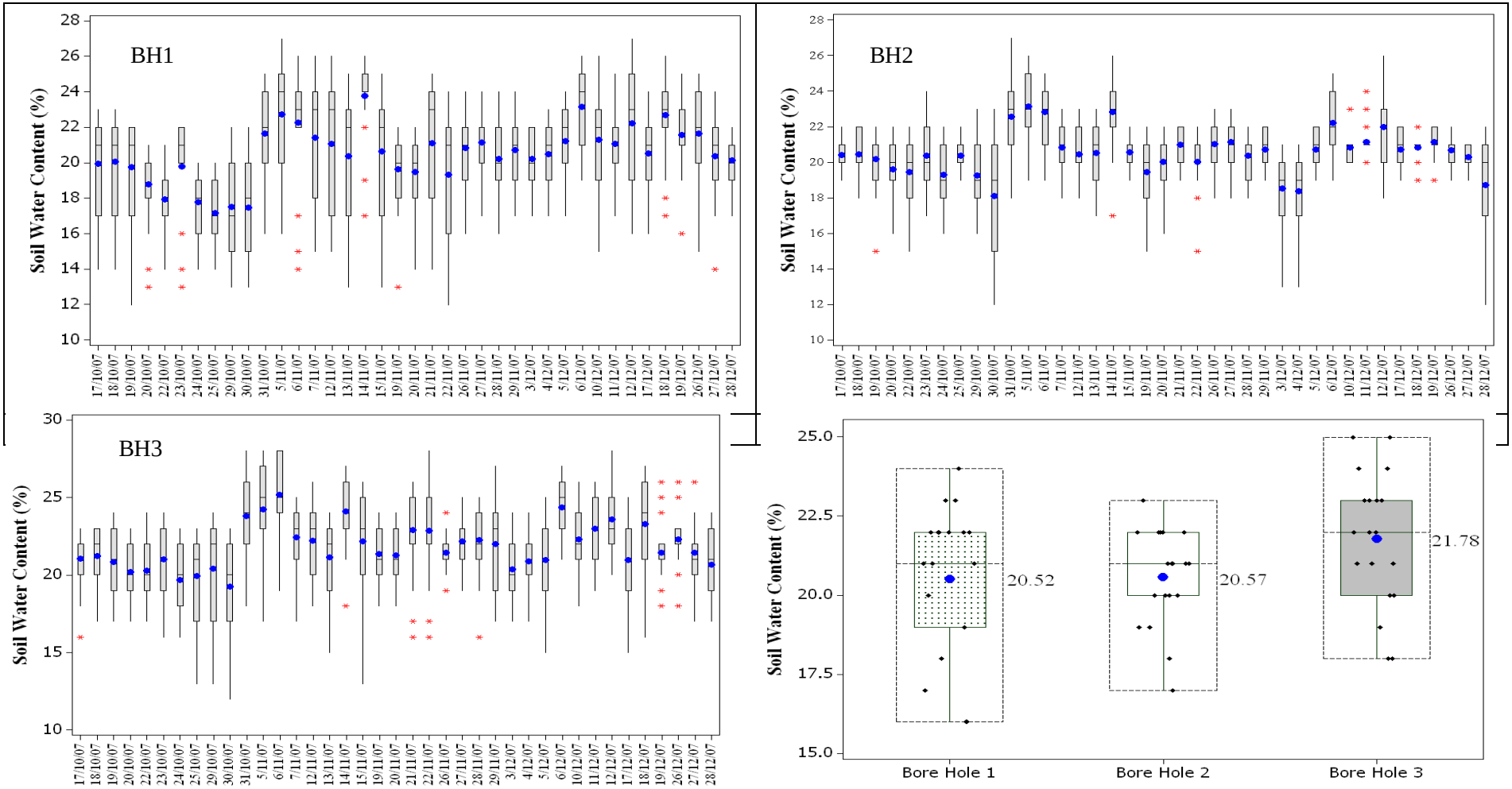

Figure 7: Distribution pattern of soil water content in box plot figures

Comparison of Soil Water Characteristics Between the Three Study Sites

In order to visualize the differences among the three NMM results obtained from BH1, BH2 and BH3, graphs 1:1 were plotted as shown in *Figure 8*. From the graphs, BH3 access tube indicated a significantly higher Θ values compared to BH1 and BH2. However, Θ values at BH1 and BH2 was equally distributed. As indicated in *Figure 8*, higher Θ values occurred for BH1 and BH2 at >1.0 m and <1.0 m of soil depth, respectively. This study also revealed that a steady increase of Θ values occurred with increment of soil depth up to 2.0 m maximum.

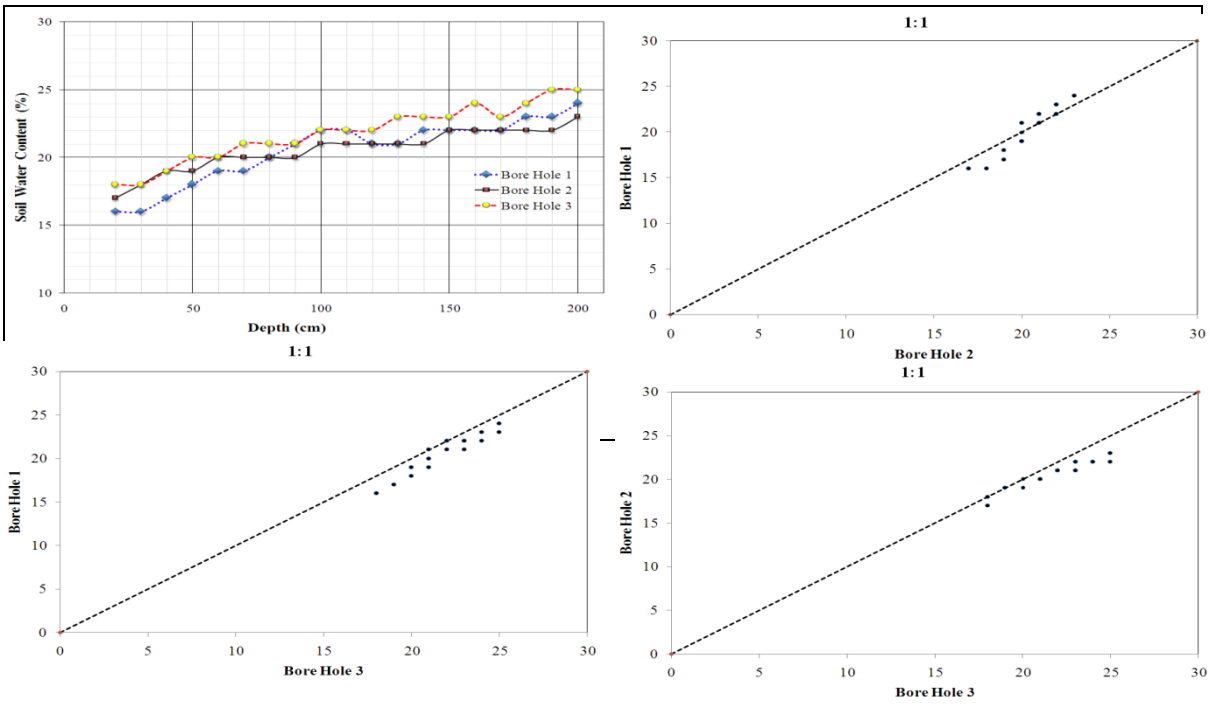

Figure 8: 1:1 graphs for BH1, BH2 and BH3 in the oil palm catchment

Further analysis revealed that an increase in Θ occurred in response to occurrence of >30.0mm total rainfall. Eight events registered Θ_w (soil water content measured within 24 h after rainfall) greater than the average Θ_d (soil water content measured during dry conditions) for all three bore holes *(Figure 9)*. Percentage Θ increment ranged from 5.0-23.8% for BH1, 4.3-31.3% for BH2 and 4.5-33.3% for BH3 when high rainfall occurred.

Our data also showed that the average travelling time for water to percolate from the surface to 1.1, 1.5, and 1.6 m depths for BH1, BH2 and BH3 respectively, was about 4-10 h. For example, after 4 h of 46.6 mm of rainfall, the water moved 1.1 m in BH1, 1.5 m in BH2 and 1.6 m in BH3. The soil water content percentage increment ranged from 9.5 to 23.8% at these particular depths. However, traveling period for water in the soil was dependent on the amount of rainfall and the antecedent conditions (Cheng *et al*. 2013). Other studies also suggest that rapid movement may occur through the upper layers and movement in deeper layers is typically slower (Lo *et al.* 2020). Our study results show that the Θ values decrease slowly in response to dry conditions when no high rainfall was recorded after 24 h from the previous storm event.

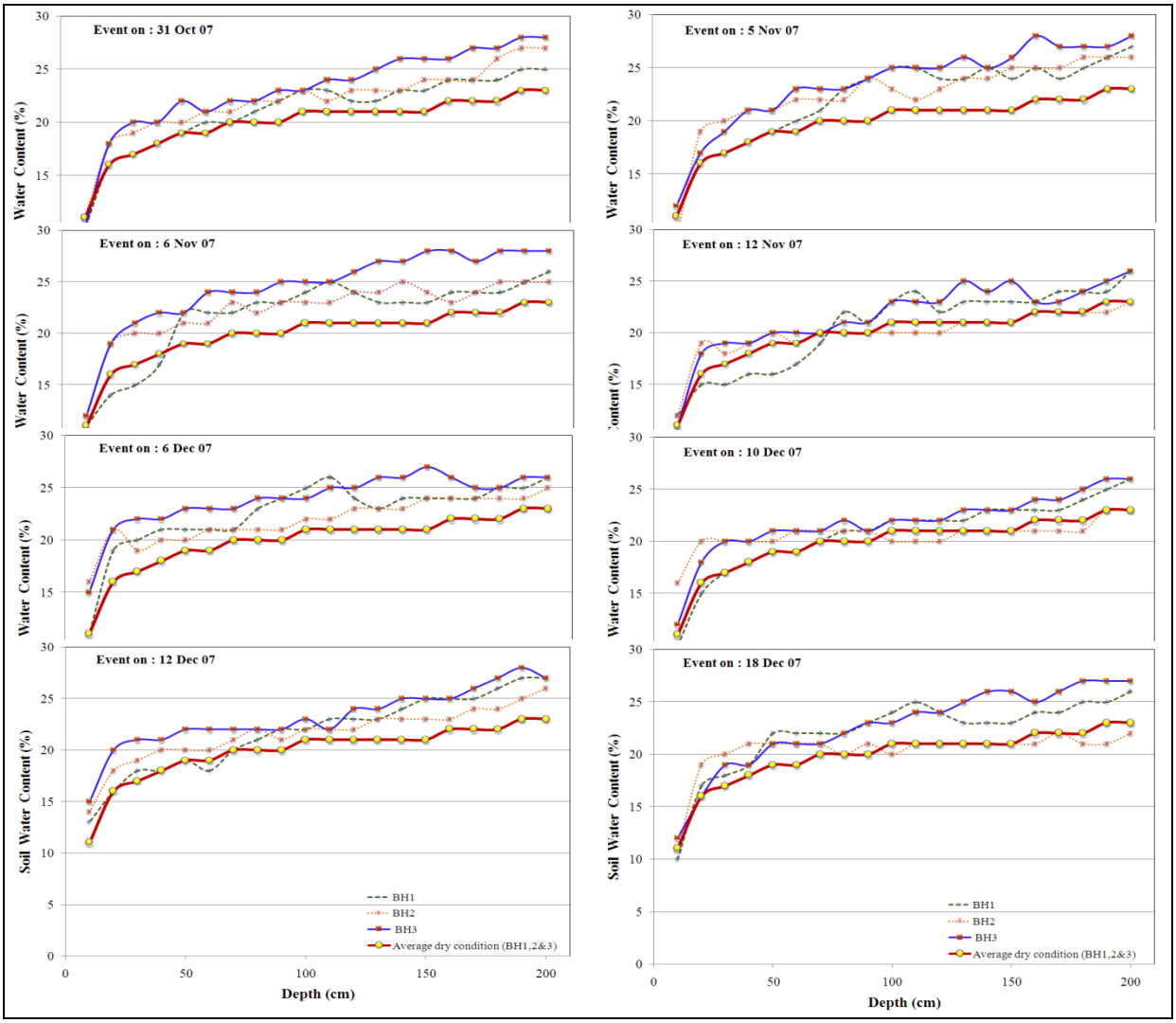

Figure 9: A significant increase in Θ_w in response to high rainfall (>30.0 mm)

Resistivity Imaging System Survey Results

Resistivity monitoring was carefully established at three study sites in accordance to RIS requirements. From the findings, all catchments exhibited high resistivity values within 6.0 m depths. The stratigraphy patterns are described according to the respective study sites

Catchment 1 (C1) Stratigraphy Pattern

The stratigraphy pattern for C1 is shown in *Figure 10*. The general characteristics of C1 according to RIS sampling:

1) Hard zone covered an area more than 40% of the total resistivity image.
2) Stream leakage occurred contributing to ground water.
3) No clear indications of shallow horizontal flow towards stream based on the groundwater contour, but possibilities of leakage of shallow horizontal flow towards ground water bearing strata.
4) Clear inter-connection among existing hard layers within the survey area.
5) Difficult to identify the inter-connection between horizontal flow and ground water bearing strata.

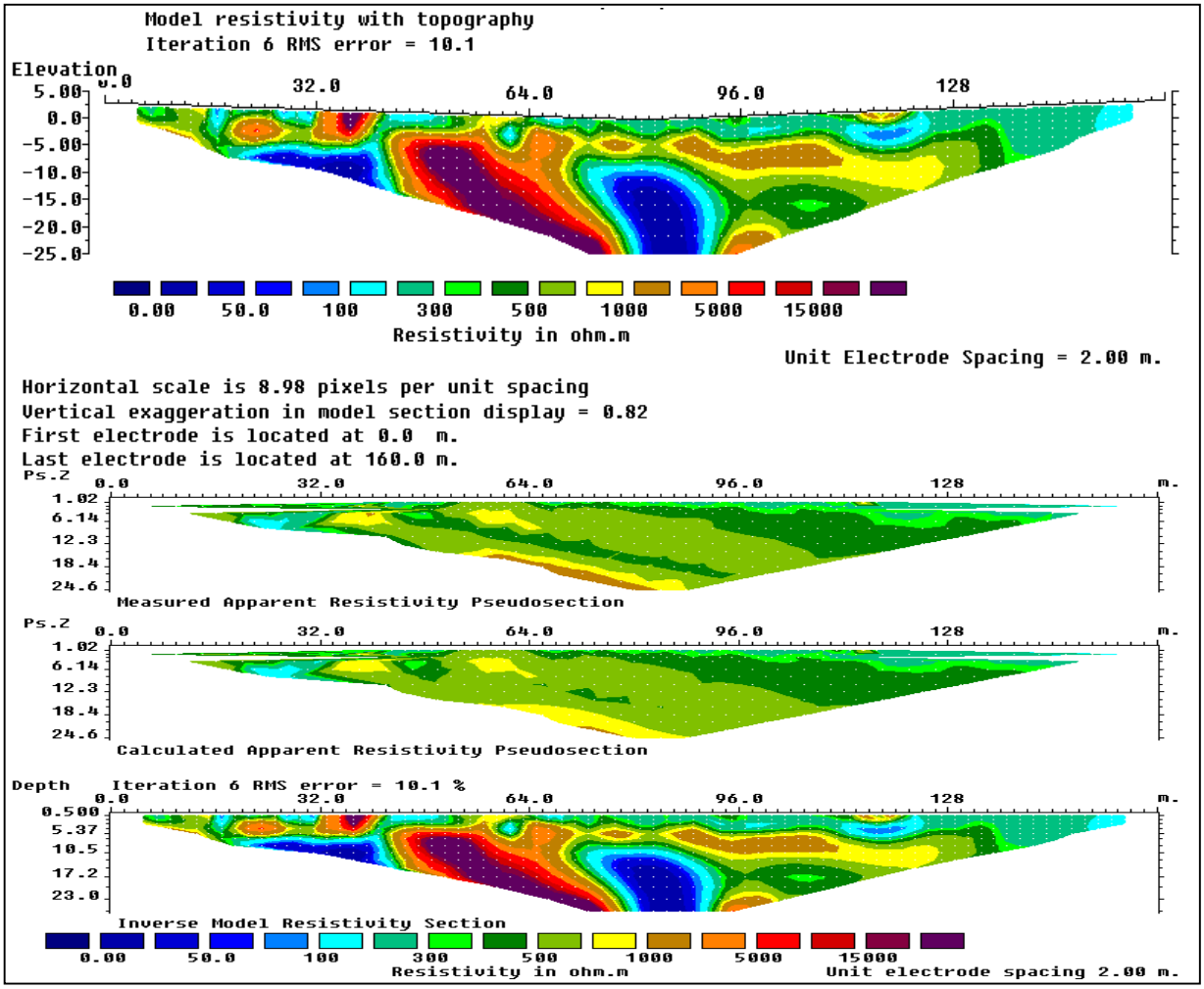

Figure 10: Resistivity imaging with topography of Catchment 1

Catchment 2 (C2) Stratigraphy Pattern

The stratigraphy pattern for C2 is shown in *Figure* 11. The general characteristics of C2 according to RIS sampling:

1) Presence of clear indications of horizontal flow towards stream
2) High permeability type of soil characteristics
3) Lack of hard zone with detection of only a few boulders.
4) No leakages of stream towards ground water.

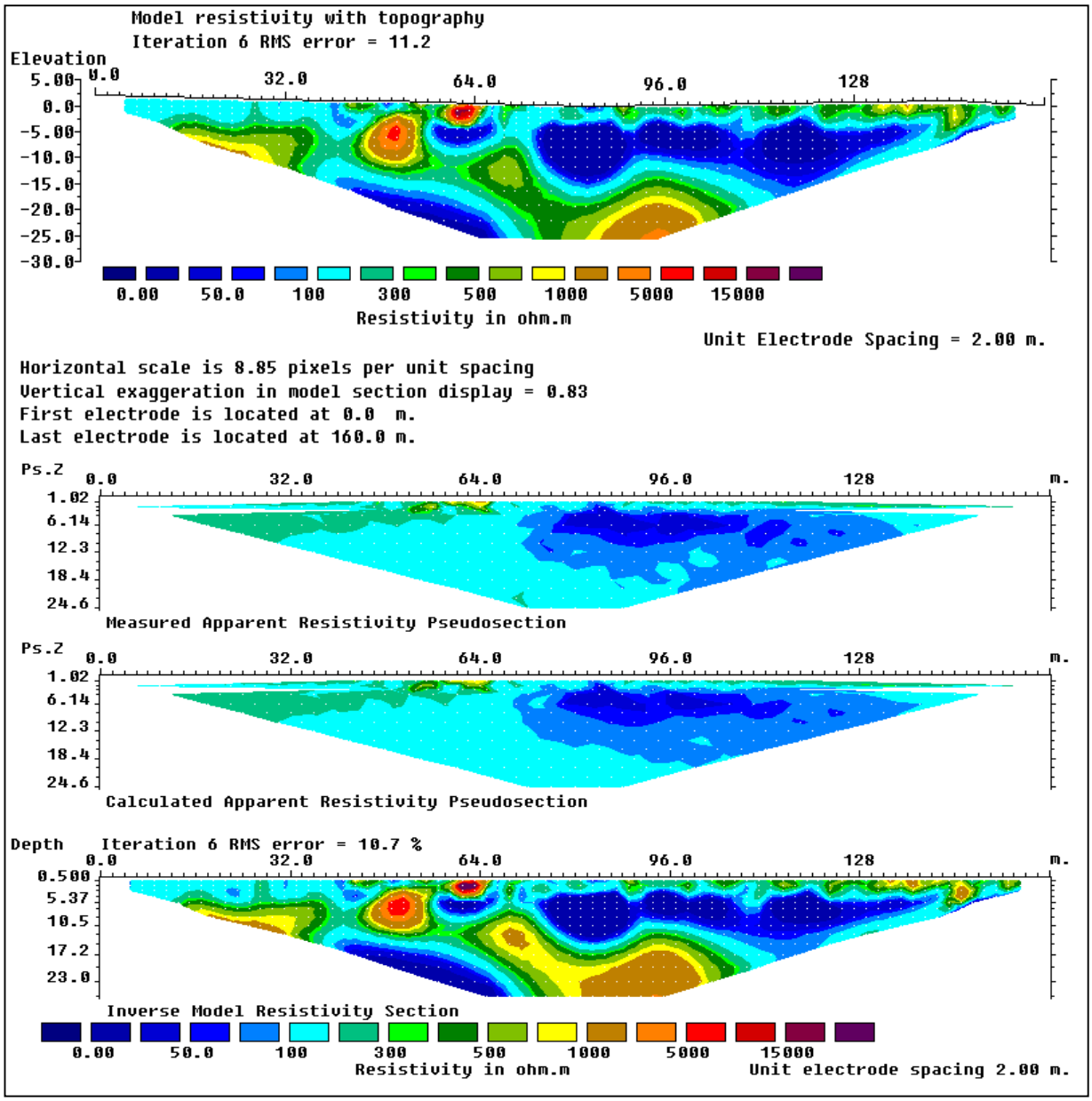

Figure 11: Resistivity imaging with topography of Catchment 2

Catchment 3 (C3) stratigraphy pattern

The stratigraphy pattern for C3 is shown in *Figure 12*. The RIS sampling found a shallow water saturated strata within 2.0 to 6.0 m depth, which reaffirmed the NMM findings where this phenomenon was observed at 1.0 to 2.0 m depth. General characteristics of C3 according to RIS sampling were:

1) Flow of subsurface water zone towards the stream based on groundwater contour.
2) High porosity zone beyond 2.0 m depth, reaffirming NMM findings.

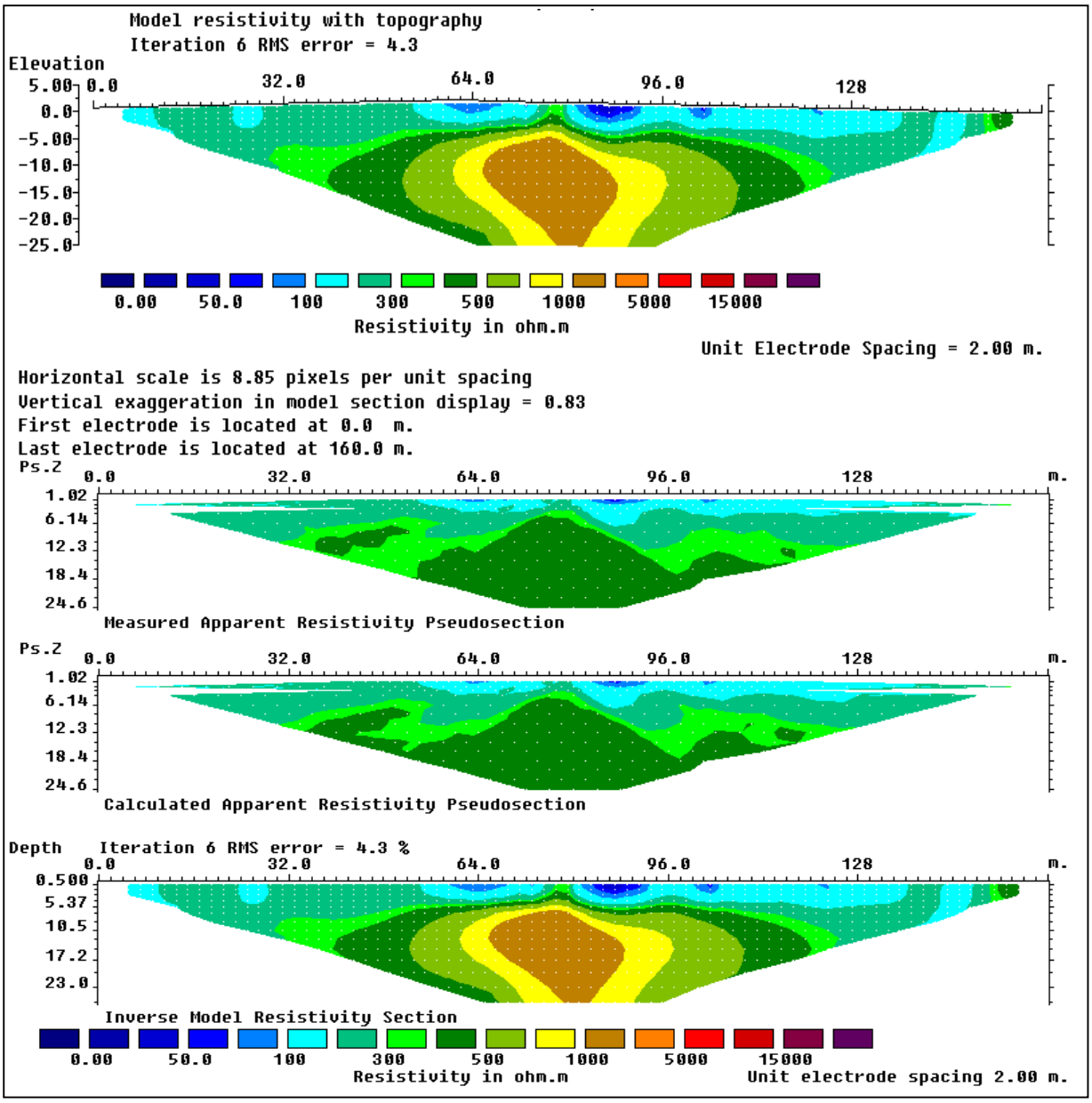

Figure 12: Resistivity imaging with topography of Catchment 3

CONCLUSION

The results obtained using NMM revealed a small significant variability in Θ values in the 20 different soil depths. Variability of soil water content also showed a significant increase in response to high rainfall events (>30.0 mm). Θ values decreased when there was no high

rainfall after 24 h and this showed that time also has an influencing role. The average travelling time for water to move from the surface to 1.1m, 1.5m, and 1.6 m for BH1, BH2 and BH3, respectively was found to be about 4-10 h. However, as measurements were not made below 2.0 m. it was not possible to determine whether preferential flow occurred at greater depths in oil palm catchments. The 2-D direct current resistivity surveys using 80-electrode imaging technique was successfully used in this study to map the soil water content underneath the oil palm catchment up to 6 m depth. The NMM and RIS analyses identified the soil characteristics that influence water behavior in the ground. Both Θ values and stratigraphy pattern showed that soil depth, rainfall intensity and antecedent conditions directly affected water flow. Though vegetative cover is known to have an effect on soil-water relationship (Dinar *et al*. 2019), our Θ values and stratigraphy pattern showed that soil depth and antecedent conditions were a bigger influencing factor in the oil palm plantations. Both techniques (NMM and RIS) were able to model the soil-water relationship in oil palm plantations and can be used in the future to charter better water management strategies in oil palm plantations.

ACKNOWLEDGEMENTS

This work was supported by Universiti Teknologi Malaysia under Research Vote No 74287. The publication of this study was funded by Universiti Putra Malaysia, under the Geran Putra Inisiatif Putra Muda (Vot 9706500) grant. The authors wish to acknowledge the Mahamurni Oil Palm Plantation Sdn Bhd for access to the Sedenak oil palm catchment and to Ms Remy, Mr Sekam and Mr Morris for their support and cooperation in this study.

REFERENCES

Ain-Lhout, F., S. Boutaleb, M. Diaz-Barradas, J. Jauregui and M. Zunzunegui. 2016. Monitoring the evolution of soil moisture in root zone system of *Argania spinosa* using electrical resistivity imaging. *Agricultural Water Management* 164: 158-166.

Anyaoha, K., R. Sakrabani, K. Patchigolla and A. Mouazen. 2018. Critical evaluation of oil palm fresh fruit bunch solid wastes as soil amendments: Prospects and challenges. *Resources, Conservation and Recycling* 136: 399-409.

Castellanos-Navarrete, A., F. de Castro and P. Pacheco. 2021. The impact of oil palm on rural livelihoods and tropical forest landscapes in Latin America. *Journal of Rural Studies* 81: 294-304.

Chanasyk, D. S. and M.A. Naeth. 1996. Field measurement of soil moisture using neutron probes. *Canadian Journal of Soil Sciences* 76: 317–323.

Cheng, Q., Y. Sun, Y. Qin, X Xue, X. Cai, W. Sheng and Y. Zhao. 2013. *In situ* measuring soil ice content with a combined use of dielectric tube sensor and neutron moisture meter in a common access tube. *Agricultural and Forest Meteorology* 171-172: 249-255.

Dinar, A., A. Tieu and H. Huynh. 2019. Water scarcity impacts on global food production. *Global Food Security* 23: 212-226.

Gonzalez-Diaz, A., A. Pataquiva-Mateus and J. García-Núñez. 2021. Recovery of palm phytonutrients as a potential market for the by-products generated by palm oil mills and refineries–A review. *Food Bioscienc*e 41:100916.

Karam, D.S., P. Nagabovanalli, K.S. Rajoo, F.C. Ishak, A. Abdu and Z. Rosli, F.M. Muharam and D. Zulperi. 2022. An overview on the preparation of rice husk biochar, factors affecting its properties, and its agriculture application. *Journal of The Saudi Society of Agricultural Sciences* 21(3): 149-159. doi: 10.1016/j.jssas.2021.07.005

Li, C., T. Jiang, X. Luan, Y. Yin, P. Wu, Y. Wang and S. Sun. 2021. Determinants of agricultural water demand in China. *Journal of Cleaner Production* 288: 125508.

Loke M.H. 2000. Electrical Imaging Surveys for Environmental and Engineering Studies. Technical note of Geotomo Software. Available on line at *http://www.geoelectrical.com*

Lo, T., D. Rudnick, J. Singh, H. Nakabuye, A. Katimbo, D. Heeren and Y. Ge. 2020. Field assessment of inter-replicate variability from eight electromagnetic soil moisture sensors. *Agricultural Water Management*: 105984.

Olaniyi, O. and K. Szulczyk. 2020. Estimating the economic damage and treatment cost of basal stem rot striking the Malaysian oil palms. *Forest Policy and Economics* 116: 102163.

Pan, Y., Q. Zhang, Y. Yu, Y. Tong, W. Wu, Y. Zhou, W. Hou and J. Yang. 2021. Three-dimensional migration and resistivity characteristics of crude oil in heterogeneous soil layers. *Environmental Pollution* 268: 115309.

Radersma, S. and C.K. Ong. 2004. Spatial distribution of root length density and soil water of linear agroforestry systems in sub-humid Kenya: implications for agroforestry models. *Forest Ecology and Management* 188: 77-89.

Rajoo, K. S., Karam, D. S., Wook, N., & Abdullah, M. 2020. Forest therapy: An environmental approach to managing stress in middle-aged working women. Urban Forestry & Urban Greening, 55, 126853. doi:10.1016/j.ufug.2020.126853

Rajoo, S.K., D.S. Karam, A. Abdu, Z. Rosli and G. James Gerusu. 2021a. Urban Forest Research in Malaysia: A Systematic Review. *Forests* 12(7): 903. doi:10.3390/f12070903

Rajoo, S. K., Singh Karam, D., Abdu, A., Rosli, Z., & James Gerusu, G. 2021b. Addressing psychosocial issues caused by the COVID-19 lockdown: Can urban greeneries help? Urban Forestry & Urban Greening, 65, 127340. doi:10.1016/j.ufug.2021.127340

Rawls, W.J., J.F. Zuzel and G.G. Schumaker. 1973. Soil moisture trends on sagebrush rangelands. *Journal of Soil Water Conservation* 28(6): 270-272.

Rucker, D., C. Tsai, K. Carroll, S. Brooks, E. Pierce, A. Ulery and C. Derolph. 2021. Bedrock architecture, soil texture, and hyporheic zone characterization combining electrical resistivity and induced polarization imaging. *Journal of Applied Geophysics* 188: 104306

Saad, M., M. Wirzal and Z. Putra. 2021. Review on current approach for treatment of palm oil mill effluent: Integrated system. *Journal of Environmental Management* 286: 112209.

Subramaniam, V. and Z. Hashim. 2018. Charting the water footprint for Malaysian crude palm oil. *Journal of Cleaner Production* 178:675-687.

Tey, Y., M. Brindal, M. Djama, A. Hadi and S. Darham. 2021. A review of the financial costs and benefits of the Roundtable on Sustainable Palm Oil certification: Implications for future research. *Sustainable Production and Consumption* 26: 824-837.

Tezara, W., T. Domínguez, D. Loyaga, R. Ortiz, V. Chila and M. Ortega. 2021. Photosynthetic activity of oil palm (*Elaeis guineensis*) and interspecific hybrid genotypes (*Elaeis oleifera* × *Elaeis guineensis*), and response of hybrids to water deficit. *Scientia Horticulturae* 287:110263.